DOI: 10.1002/hlca.201900047

HELVETICA chimica acta

Transannular Hydrogen Bonding in Planar-Chiral [2.2] Paracyclophane-Bisamides

Will R. Henderson,[a] Danielle E. Fagnani,[a] Jonathan Grolms,[a] Khalil A. Abboud,[a] and Ronald K. Castellano*[a]

[a] Department of Chemistry, University of Florida, PO Box 117200 Gainesville, FL 32611–7200, USA,
e-mail: castellano@chem.ufl.edu

Dedicated to Prof. *François Diederich* on the occasion of his retirement

A series of [2.2]paracyclophane-bisamide regioisomers and alkylated comparators were designed, synthesized, and characterized in order to better understand the transannular hydrogen bonding of [2.2]paracyclophane-based molecular recognition units. X-Ray crystallography shows that transannular hydrogen bonding is maintained in the solid-state, but no stereospecific self-recognition is observed. The assignment of both transannularly and intermolecularly hydrogen bonded N- H stretches could be made by infrared spectroscopy, and the effect of transannular hydrogen bonding on amide bond rotation dynamics is observed by ^{1}H-NMR in nonpolar solvents. The consequences of transannular hydrogen bonding on the optical properties of [2.2] paracyclophane is observed by comparing alkylated and non-alkylated *pseudo-ortho* 4,12-[2.2]paracyclophane-bisamides. Finally, optical resolution of 4-mono-[2.2]paracyclophane and *pseudo-ortho* 4,12-[2.2]paracyclophane-bisamides was achieved through the corresponding sulfinyl diastereoisomers for circular dichroism studies. Transannular hydrogen bonding in [2.2]paracyclophane-amides allows preorganization for self-complementary intermolecular assembly, but is weak enough to allow rapid rotation of the amides even in nonpolar solvents.

Keywords: chirality, cyclophanes, hydrogen bonds, self-assembly, supramolecular chemistry.

Introduction

[2.2]Paracyclophane (**[2.2]pCp**) is a classically interesting hydrocarbon that has fostered a better understanding of chromophore interactions, aromaticity, and stereochemistry for well over a half-century.[1] Its utility comes from the proximity and non-planarity of its 'bent and battered benzene rings'[2–4] and rigid, structurally defined skeleton. The limited mobility and rotation of the bridging atoms and benzene 'decks' can lead to planar chirality in certain substituted **[2.2]pCps**, while the two phenyl rings are electronically coupled both through-bond [σ(bridge)–π(deck)] and through-space (transannular π–π) to perturb the molecule's chemical, electronic, and optical properties.[5–15] The large body of synthetic methodology reported for **[2.2]pCps** allows chemists to efficiently synthesize and selectively functionalize them,[16–20] generating derivatives for broad application including as ligands and catalysts,[21,22] as well as π-conjugated oligomers and polymers.[23–29]

Despite a rich history in supramolecular chemistry for cyclophanes,[30–33] **[2.2]pCp** has been relatively unexplored in a supramolecular context, except for a few excellent reports.[34–36] Recently, our group published the first example of a self-complementary **[2.2]pCp** H-bonding unit capable of forming a supramolecular polymer whose helical sense is dictated by the planar chirality of the monomer (*Scheme 1*).[37] This system is based on 4,7,12,15-[2.2]-paracyclophane-tetraamide (**[2.2]pCpTA**) which self-assembles in nonpolar solvents through inter- and intramolecular (transannular) hydrogen bonding be-

Supporting information for this article is available on the WWW under https://doi.org/10.1002/hlca.201900047

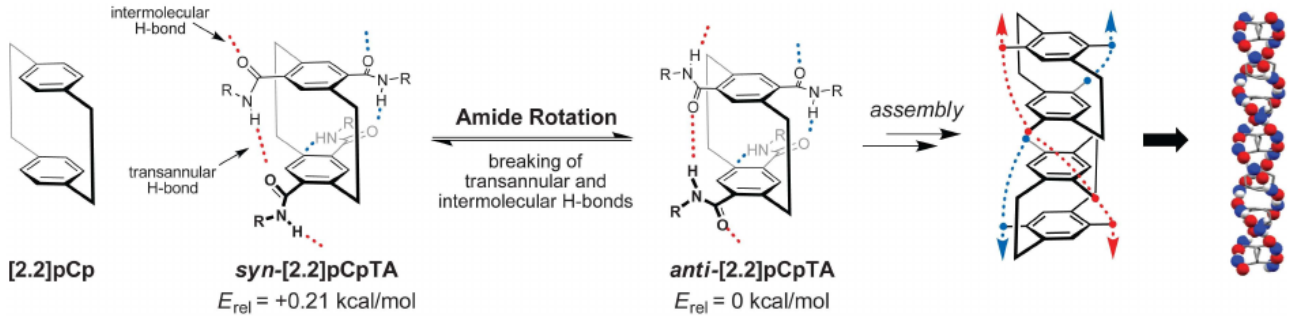

Scheme 1. Self-assembly of 4,7,12,15-[2.2]paracyclophane-tetraamide (**[2.2]pCpTA**) promoted by transannular and intermolecular hydrogen bonding (see ref. [37] for details). Only the (S_p)-configuration of the **[2.2]pCpTA** monomer is shown for simplicity. The relative conformer energies have been obtained from DFT calculations at the M06-2X/6-31G* level of theory. Also shown is a portion of the X-ray crystal structure of ***anti*-[2.2]pCpTA** with atoms involved in H-bonding depicted as enlarged spheres, and alkyl chains omitted for clarity.

tween the two pairs of *para*- and *pseudo-ortho* positioned amides. The design of **[2.2]pCpTA** exploits pre-organization of amides for intermolecular hydrogen bonding through a combination of steric interactions with the alkyl bridge (reminiscent of *Nuckolls*' 'crowded BTAs'[38]) and transannular hydrogen bonding to 'pre-pay' the entropic cost associated with self-assembly. Intramolecular hydrogen bonding is a common recipe for pre-organization[39] in other supramolecular systems including oligopeptides,[40] foldamers,[41] and calixarenes.[42–46] The approach generally reduces degrees of freedom and decreases the dynamics of molecular recognition units,[47] substantially strengthening association constants.[48] Although several examples of **[2.2]pCp**-based planar-chiral catalysts and ligands capable of transannular H-bonding have been reported,[49–53] there has not been an effort to understand the effects of transannular H-bonding on **[2.2]pCp** structure and properties. Specifically understanding the relative strength and geometry of transannular H-bonding in the **[2.2]pCpTA** assembly motif, and its effects on molecular self-recognition, are critical to rationally design the next generation of **[2.2]pCp**-based supramolecules.

The conformational complexity introduced to **[2.2]-pCpTA** by transannular hydrogen bonding is expected to significantly affect its molecular and supramolecular properties. Two important **[2.2]pCpTA** conformers (*syn*- and *anti-)*, while close in energy as monomers, differ in their H-bonding arrangements and assembly macrodipoles, presumably leading to different self-association constants (*Scheme 1*). The two conformers can only associate with themselves (*syn*- with *syn*- and *anti*- with *anti-)* but can be interrelated by the rotation of two *pseudo-ortho* positioned amides, which would involve breaking one transannular H-bond, and up to two intermolecular H-bonds with **[2.2]pCpTA** neighbors. If the interconversion between the conformers is slow compared to the time-scale of assembly in solution, it can lead to competing assembly pathways with different association strengths corresponding to both *syn*- and *anti*-assemblies and therefore, a non-equilibrium supramolecular polymer.[54] Computational data suggests that the *anti*-conformer is the predominant assembling species, but both conformers will exist in solution.[55] We envision that the two conformers, because of their structural similarities and electronic differences, will be useful models for understanding structure- mechanism relationships in supramolecular polymers.[56]

Reported here are the design, synthesis, and investigation of simpler disubstituted **[2.2]pCp** systems to closely examine transannular H-bonding independent of strong intermolecular assembly (*Figure 1*). In addition to understanding the influence of transannular hydrogen bonding on amide rotation dynamics, comparator compounds should also help to understand the impact of amide substitution on structural and chiroptical properties of such **[2.2]pCps**. The characterization – by single crystal X-ray analysis, NMR, IR, UV/Vis, and CD spectroscopy – assigns structural and spectral characteristics of the **[2.2]-pCpTA** self-assembly motif, furthers the understanding of amides involved in pCp transannular hydrogen bonding, and allows the prediction of pathway selection in the equilibrium supramolecular polymerization of **[2.2]pCpTA**.

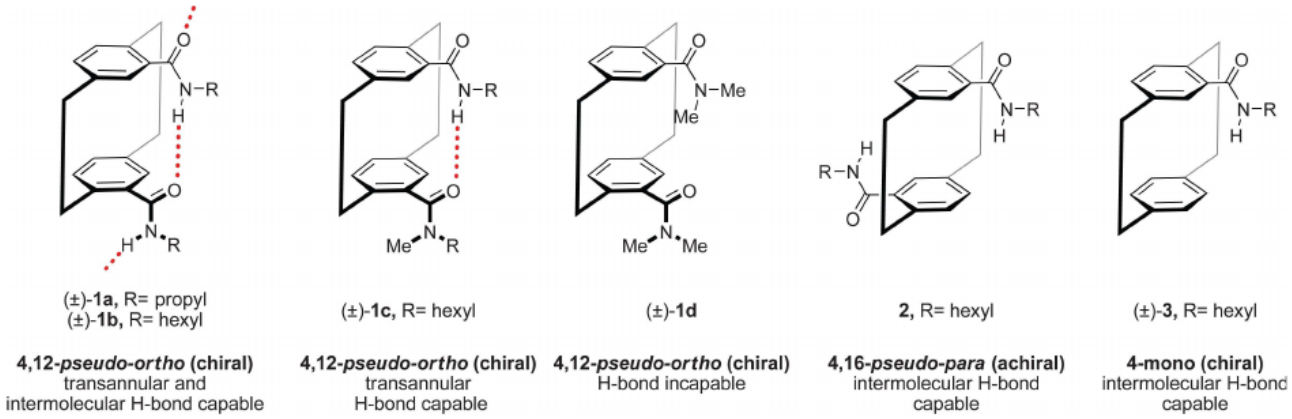

Figure 1. The **[2.2]pCp**-bisamide compounds studied in this work. Chiral compounds shown in the (R_p)-configuration. Only one amide rotamer shown for compound (±)-**1c**.

Results and Discussion

Design

The small library of regioisomeric **[2.2]pCp**-bisamides and alkylated comparators studied in this work (*Figure 1*) were chosen to control transannular and intermolecular hydrogen bonding sufficient to examine the interplay between the two modes of H-bonding and understand how they likely affect **[2.2]-pCpTA** molecular recognition. Out of the four readily accessible disubstituted **[2.2]pCps**, only the *pseudo-gem* 4,13-**[2.2]pCp** (ps-*gem*) and the *pseudo-ortho* 4,12-**[2.2]pCp** (ps-*o*) are capable of forming transannular H-bonds, and of these, only the ps-*o* regioisomer is chiral. We have examined transannular hydrogen bonding capable ps-*o* **[2.2]pCp**-bisamides in the solid state through X-ray crystallography and in solution by ^{1}H-NMR, IR, and UV/Vis. As for the amide substituents (R), hexyl chains were chosen for (±)-**1b**, **2**, and (±)-**3** to allow solution studies, while a propyl chain was chosen for crystal growth and analysis of compound (±)-**1a**. Alkylated model compound (±)-**1c** would be incapable of intermolecular hydrogen bonding, and was used to examine the effects of transannular H-bonding on the solution properties of **[2.2]pCp** amides. Completely H-bond incapable bis-tertiary amide compound (±)-**1d** is an appropriate compound to study the electronic properties of ps-*o* bisamides in the absence of transannular H-bonding. Comparison of (±)-**1d** with (±)-**1b** can then attribute the different electronic signatures primarily to transannular H-bonding because of the electronic and symmetry (C_2) similarities between (±)-**1b** and (±)-**1d**. The *pseudo-para* 4,16-**[2.2]pCp** (ps-*p*) bisamide compound **2**, with two amides capable of intermolecular H-bonding, but without transannular H-bonding, could be used to examine the role of transannular H-bonding in self-assembly. Monosubstituted compound (±)-**3** as an amide substituted **[2.2]pCp** that is planar-chiral, but incapable of transannular H-bonding, can help explore the effect of transannular H-bonding on chiroptical properties of amido-**[2.2]pCps**.

Synthesis and Chiral Resolution

The synthetic approach to **[2.2]pCp**-bisamide targets (±)-**1a**–(±)-**1d** and **2** followed the general approach of electrophilic bromination and isomer interconversion of commercially available **[2.2]pCp**[16] (*Scheme S1*), followed by lithium-halogen exchange and quenching with gaseous CO_2 to yield the carboxylic acid derivatives (±)-**4** and **5** (*Scheme S1*). Amide bond formation was achieved through an acyl chloride intermediate followed by condensation with a primary amine to give ps-*o*-bisamides (±)-**1a** and (±)-**1b** (*Scheme 2*). Alkylated ps-*o*-bisamide model compound (±)-**1c** was synthesized in one step by reacting compound (±)-**1b** with 1.5 equivalent NaH and MeI to give selectively mono-alkylated compound (±)-**1c**. In the preparation of (±)-**1c**, no bis-alkylated product was observed. This could mean that the transannular H-bond controls selectivity by making the second amide N- H, on the opposite dec from the tertiary amide, less reactive towards alkylation even in highly polar, H-bond accepting solvents such as DMF. Condensation of the acyl chloride of (±)-**4** with dimethylamine gives fully alkylated **[2.2]pCp**-bis(tertiary)amide (±)-**1d**. Amide bond formation occurs from **7** in similar yields as (±)-**1b** to give ps-*p*-bisamide **2**.

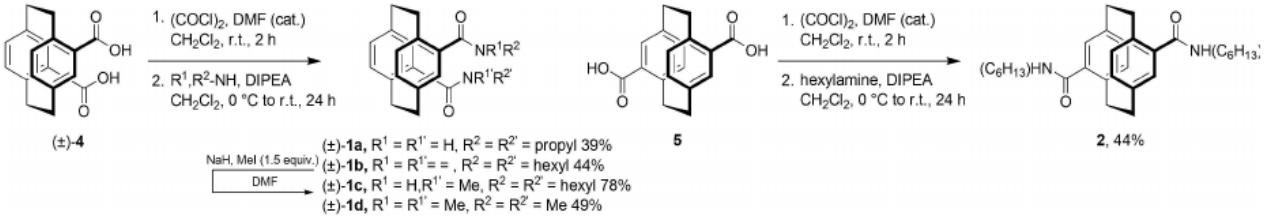

Scheme 2. Synthesis of ps-*o*-bisamide compounds (±)-**1a**–(±)-**1d**, and ps-*p*-bisamide **2**.

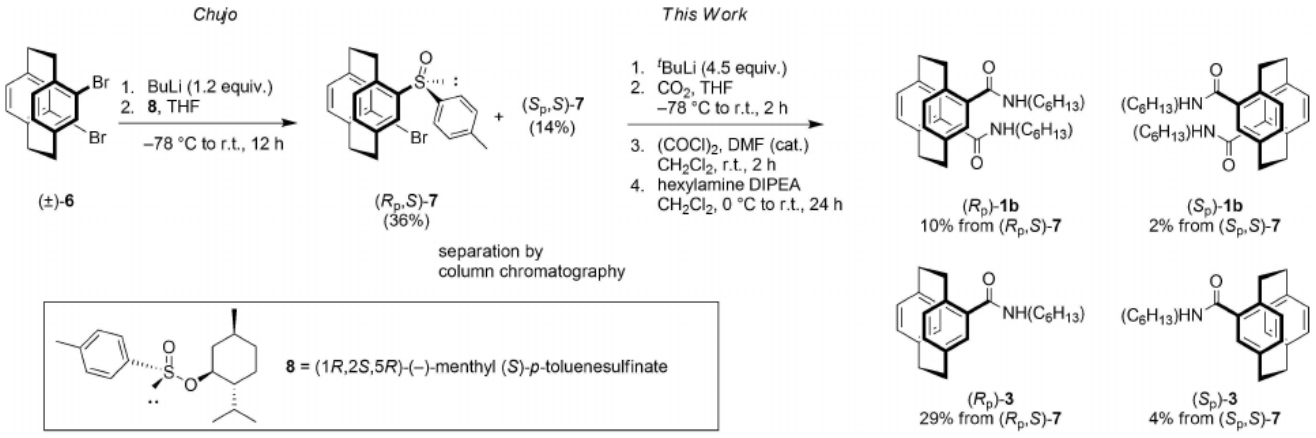

Scheme 3. Chiral resolution as described by *Chujo* and coworkers gives key sulfinyl diastereoisomers (S_p,*S*)-**7** and (R_p,*S*)-**7**, which could be subjected to carboxylation and amide bond formation to yield enantioenriched **1b** and **3**.

The approach we chose for the chiral resolution of **[2.2]pCp**-bisamides is based on the work of *Chujo* and coworkers (*Scheme 3*).[57] This resolution proceeded with one extra synthetic step from the ps-*o*-dibromide (±)-**6**. Lithiation of (±)-**6** with 1.2 equivalents BuLi and quenching with (1*R*,2*S*,5*R*)-(-)-menthyl (*S*)-*p*-toluenesulfinate (**8**) gives sulfinyl diastereoisomers (R_p,*S*)-**7** and (S_p,*S*)-**7**, which can be separated by silica gel chromatography. *Chujo* and coworkers showed that upon lithiation of (R_p,*S*)-**7** or (S_p,*S*)-**7** with ^{t}BuLi, diverse electrophiles could be introduced in good yields. Quenching of the lithiated intermediates with CO_2 as an electrophile worked to give both enantioenriched ps-*o* diacid and monoacid, although in worse yields than reported for other electrophiles (the latter is presumably a side product arising from protonation of the lithiated intermediate). This mixture was used without purification to give both enantioenriched monoamides **3** (R_p: 98% e.e., S_p: 93% e.e.) and ps-*o* bisamides **1b** (R_p: 96% e.e., S_p: 81% e.e.) after amide bond formation and separation through silica gel chromatography. With this chiral resolution strategy established, we are optimistic that it can be extended to the **[2.2]pCpTA** system.

X-Ray Crystallographic Analysis of (±)-**1a**

Slow evaporation of a methanol solution of (±)-**1a** provided colorless plates of sufficient quality for single crystal X-ray diffraction (*Figure 2*). Notably, the transannular H-bond between the amide C=O and N- H is maintained in the solid state, although the N···C=O distance (N_1···O_2) is slightly longer than that of **[2.2]pCpTA** (2.90 Å *vs.* 2.81 Å). The peripheral amide C=O and N- H bonds separately engage in intermolecular H-bonds with methanol (O_1···O_3 distance of 2.72 Å, N_2···O_3 distance of 2.87 Å). The transannular H-bond (N_1···O_2) in the crystal structure of (±)-**1a** is also closer than the distance determined from DFT calculations (2.95 Å).[37] Both enantiomeric units of (±)-**1a** are present in the unit cell, sharing intermolecular hydrogen bonds with methanol, as the methanol acts as both H-bond donor and acceptor. Twisting of the bridge methylenes of (±)-**1a** (C_{14}- C_1- C_2- C_3 dihedral = 24°) is larger than that in other H-bonding pCp systems,[34][58] but smaller than those which are covalently linked in the 4- and 12-positions.[59] A testament to the rigidity of the **[2.2]pCp** scaffold, the distances between the ps-*gem* aromatic carbons *ortho*- and *para*- to the amides are similar (C_{13}···C_4 = 3.08 Å

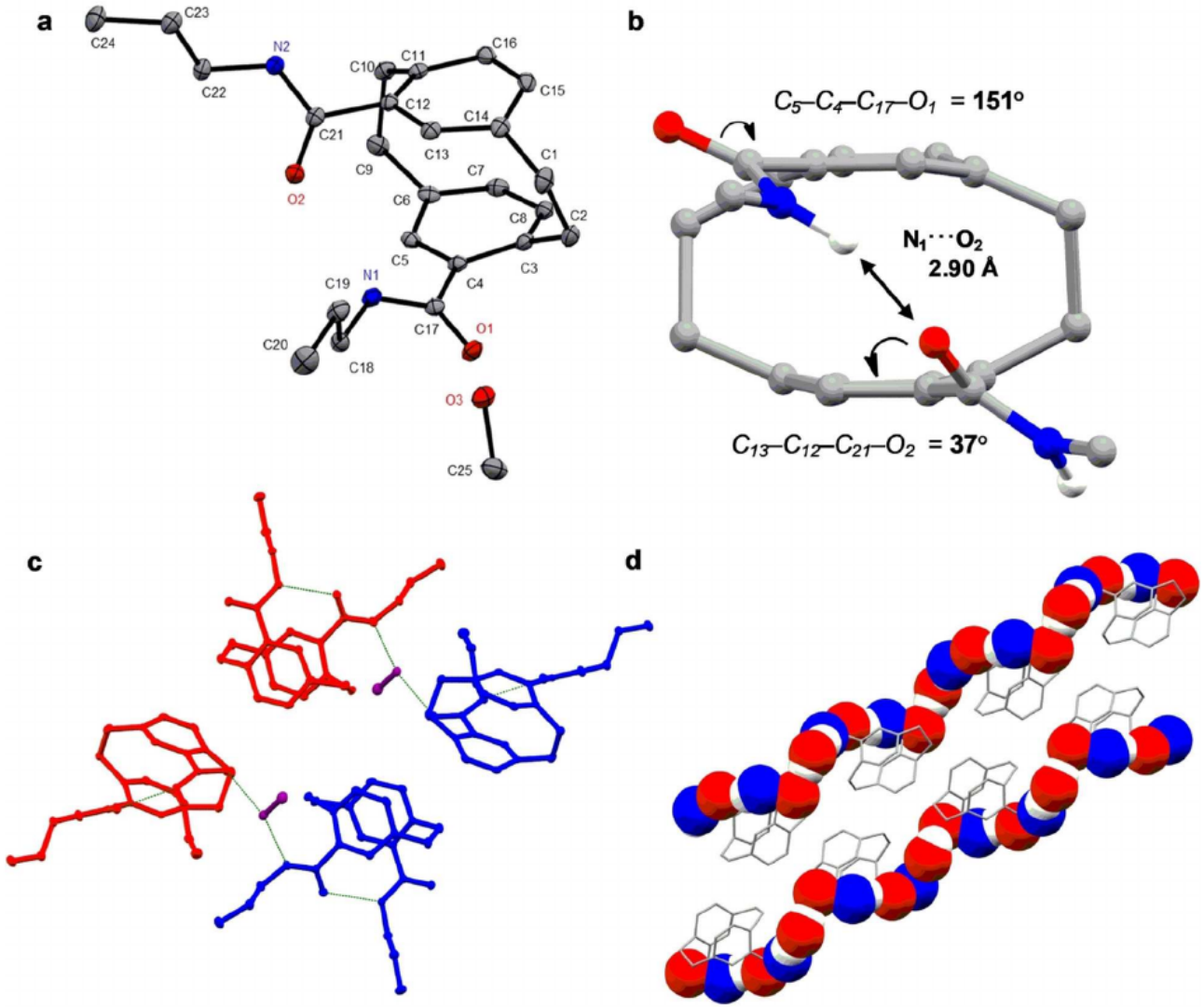

Figure 2. a) ORTEP plot of (S_p)-**1a** and atom labels, including propyl side chains and one molecule of methanol. b) Side view of (S_p)-**1a** showing dihedral angles and transannular hydrogen bonding for amides (side chains omitted for clarity). c) Unit cell of (±)-**1a** in the solid state, with (R_p)-**1a** (red), (S_p)-**1a** (blue), MeOH (purple), and hydrogen bonding (green). d) Hydrogen bond propagation through the crystal of (±)-**1a**. Atoms participating in H-bonds are shown as larger spheres for clarity. Alkyl chains have been omitted for clarity. Atom color code: blue N, gray C, red O.

and $C_{15}\cdots C_8 = 3.11$ Å), with transannular hydrogen bonding bringing the two phenyl decks slightly closer (*Figure S26*). Amide dihedrals (C_{13}- C_{12}- C_{21}- O_2) of - 37° and (C_5- C_4- C_{17}- O_1) 151° show the amides tilted out of the plane of the arene ring to a slightly lesser extent than the amides of **[2.2]pCpTA** (average dihedrals of - 38° and 141°) but comparable to calculated values.[37] Single crystals of (±)-**1a**, while produced in an identical manner (slow evaporation of a methanol solution) to **[2.2]pCpTA**, show no evidence for stereospecific intermolecular associations in the solid state (the **[2.2]pCpTA** system exhibits homochiral stacks (R_p only assembles with R_p, and S_p only with S_p) through two-fold intermolecular hydrogen). The absence of stereospecific assembly for (±)-**1a** indicates that there is a need for a second intermolecular hydrogen bond to provide this level of stereochemical instruction. The observation is consistent with the 'three-point attachment model', where the three points would consist of two intermolecular hydrogen bonds, and one π–π interaction.[60]

^{1}H-NMR Spectroscopy

Comparison of the ^{1}H-NMR spectra of compounds (±)-**1b**, (±)-**1c**, and **2** can give insight into the dynamics of

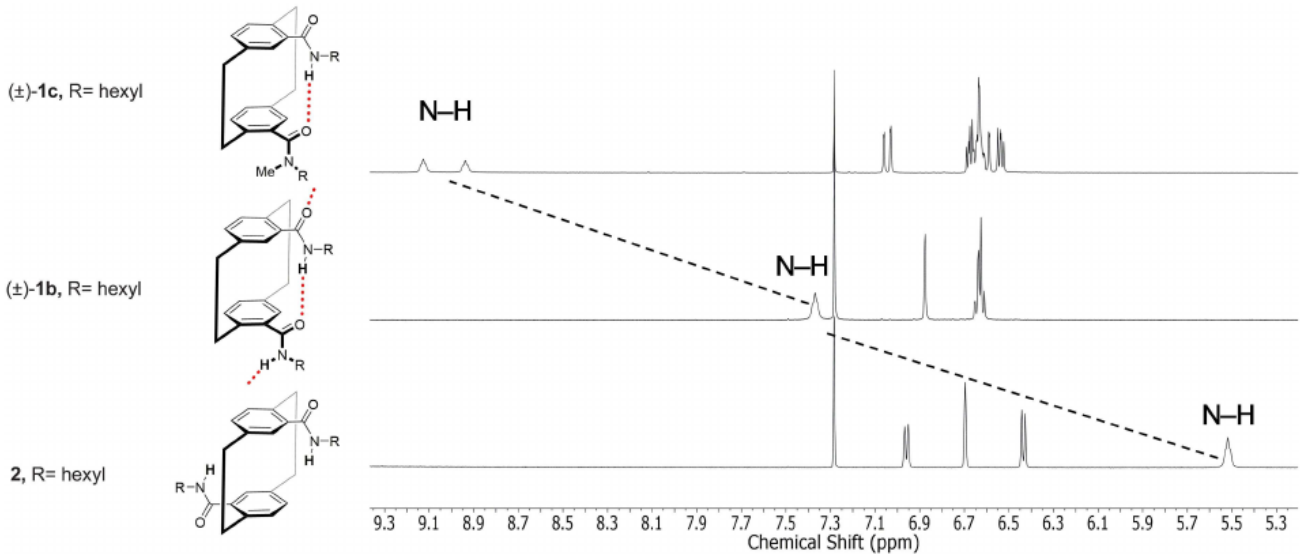

Figure 3. ^{1}H-NMR data for compounds (±)-**1b** (6 mM), (±)-**1c** (12 mM), and **2** (6 mM) in $CDCl_3$ at 298 K. The dotted line shows the trend in the position of the amide N- H resonance as it changes from bottom to top: solvent-exposed N- H, solvent-exposed and transannularly H-bonded, transannularly H-bonded only.

C_5- C_4- C_{17}- O_1 bond rotation and how it is affected by transannular H-bonding. For compound **2** in $CDCl_3$, the amide N- H chemical shift ($\delta = 5.5$ ppm) is the same as monoamide (±)-**3**,[37] and is in a solvent exposed environment. This resonance becomes deshielded in compound (±)-**1b** ($\delta = 7.3$ ppm) as a result of transannular H-bonding (*Figure 3*), and further shifts in compound (±)-**1c** ($\delta = 9.0$ ppm) as the amide N- H becomes persistently H-bonded on the NMR timescale due to the blocking of the amide N- H donor on the opposite deck by introduction of a methyl group. The amide N- H in (±)-**1c** splits into two peaks because of transannular H-bonding to an unsymmetrical tertiary amide, with the more deshielded signal ($\delta =$ 9.1 ppm) likely corresponding to the amide where the methyl group is *trans* to the carbonyl, providing less steric hindrance with the **[2.2]pCp** skeleton allowing for optimized transannular H-bonding. Interestingly, the chemical shifts of the H-bond incapable N- H in **2** and the permanently H-bonded N- H in (±)-**1c** average to the N- H chemical shift in (±)-**1b**, indicating that the N- H resonance in (±)-**1b** is the time-average of solvated and H-bonded N- H as rotation of the C_5- C_4- C_{17}- O_1 bond is fast on the NMR time-scale.

Alternatively, solutions of (±)-**1b** in nonpolar (D_{12})-cyclohexane show some concentration dependence from 1–30 mM indicating the formation of undefined aggregates (*Figure S2*). Variable temperature ^{1}H-NMR studies of (±)-**1b** as a 21 mM solution in (D_{12})-cyclohexane show the amide N- H resonance becoming deshielded ($\delta = 7.4$ ppm at 345 K to $\delta = 8.8$ ppm at 283 K, $\Delta\delta = 1.4$ ppm) with decreasing temperature, while still maintaining a defined line shape of the amide N- H (*Figure S3*). The single amide N- H resonance indicates that C_5- C_4- C_{17}- O_1 bond rotation is still fast on the NMR timescale, while the chemical shift change indicates that there is an increase in intermolecular hydrogen bonding upon lowering the temperature. There is also a change in the Ar- H protons ($\Delta\delta = 0.1$ ppm), as they become shielded at lower temperatures, suggesting an assembly similar to the one observed in **[2.2]pCpTA**, in which intermolecular amide hydrogen bonding in (±)-**1b** can be accompanied by a partial overlap of the aromatic systems in a slip-stacked fashion.

Infrared Spectroscopy

Characterization of hydrogen bonding compounds with IR spectroscopy gives insight into the behavior of individual H-bonding energies in different solvents. In more polar solvents, such as chloroform, intermolecular H-bonding is expected to be weak due to favorable solvent–solute interactions, while in nonpolar solvents like cyclohexane or methylcyclohexane, intermolecular H-bonds are expected to be stronger. This technique was previously used to confirm the lower-energy, fully hydrogen bonded amide N- H (3222 cm^{-1}) and lack of higher-energy, solvated N- H (3437 cm^{-1}) in **[2.2]-pCpTA** at even low concentrations in cyclohexane.[37]

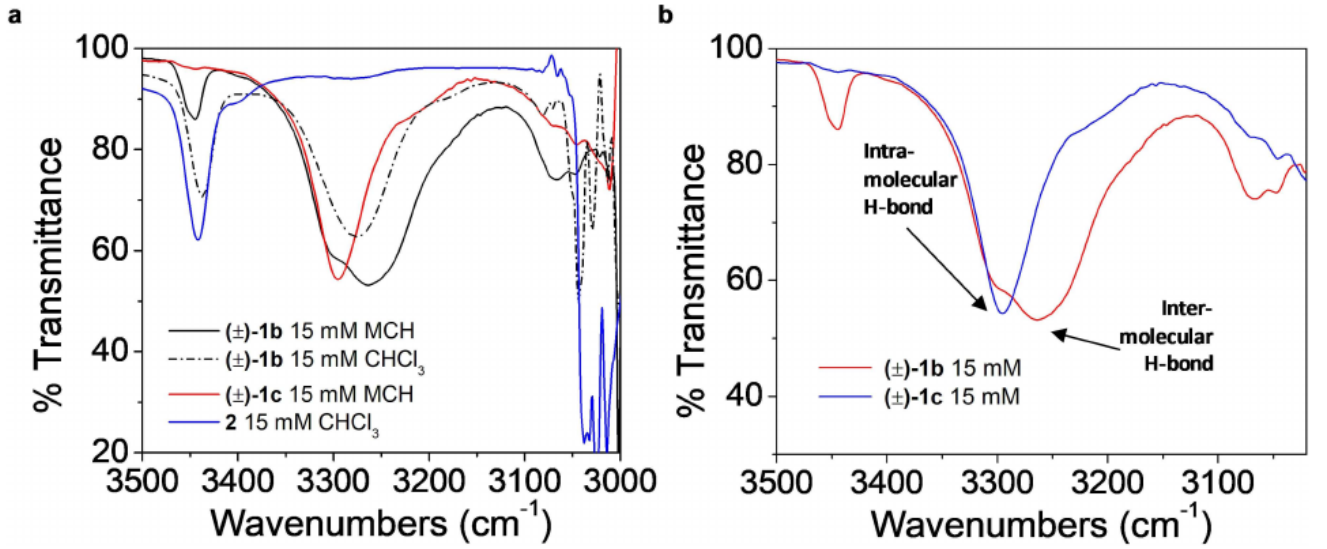

Figure 4. a) Overlaid FT-IR of (±)-**1b**, (±)-**1c**, and **2**, in $CHCl_3$ and MCH (15 mM) at 298 K. b) Solution-phase FT-IR of (±)-**1b** and (±)-**1c** (15 mM) in MCH at 298 K.

Compound (±)-**1b** can form transannular and intermolecular hydrogen bonds, but in more polar solvents like chloroform, there is only the appearance of a solvated N- H at 3437 cm^{-1} and a transannularly H-bonded N- H at 3276 cm^{-1} (*Figure 4,a*). The strong peak that occurs from 3080–3060 cm^{-1} can be assigned as an unusually high energy C- H stretch.[61] In a nonpolar solvent such as methylcyclohexane (MCH), compound (±)-**1b** exhibits a small shoulder on the H-bonded N- H peak. Comparison with non-intermolecular H-bond capable comparator (±)-**1c** allows assignment of the shoulder as the transannularly H-bonded N- H (3295 cm^{-1}), with the lower energy stretch therefore belonging to the intermolecularly H-bonded N- H (*Figure 4,b*). This intermolecularly H-bonded N- H has a concentration dependence in methylcyclohexane (*Figure S20*), shifting to lower wavenumbers with an increase in concentration (3264 cm^{-1} at 15 mM to 3249 cm^{-1} at 30 mM). This behavior is consistent with the ^{1}H-NMR data of (±)-**1b** in (D_{12})cyclohexane, as an increase in concentration or decrease in temperature leads to a shift to higher frequency and provides further evidence for intermolecular association of (±)-**1b** at millimolar concentrations.

UV/Vis Spectroscopy

The optical properties of a variety of **[2.2]pCps** have been examined through UV/Vis absorbance spectroscopy, especially those containing electron-rich donor and electron-poor acceptor groups.[62][63] Based on the proximity of the **[2.2]pCp** phenyl decks, information can be obtained about the electronic communication and delocalization of **[2.2]pCp** and appended chromophores.[64][65] The effect of transannular hydrogen bonding on the optical properties of ps-*o*-bisamides was examined using UV/Vis absorbance spectroscopy by comparing appropriate ps-*o*-bisamides. Transannular H-bond capable compound (±)-**1b** and similarly C_2-symmetric H-bond incapable compound (±)-**1d** were compared in methylcyclohexane. Linear *Beer–Lambert* plots (*Figures S6*, *S8*) indicate that these compounds do not aggregate at micromolar concentrations. Both compounds have a similarly structured band and shoulder in the far UV region (200–240 nm), but compound (±)-**1b** has a distinctly sharper peak in the region of the 'cyclophane band' (260–290 nm) which has been attributed to the overlap between the two phenyl decks (*Figure 5*).[64] This could result from a stronger transition dipole in compound (±)-**1b**, where transannular hydrogen bonding results in a permanent dipole from one deck to another, compared to compound (±)-**1d** which does not have a large persistent dipole.

Circular Dichroism Spectroscopy

Inherently chiral paracyclophanes have been well studied with regards to their chiroptical properties[66][67] and protonation studies of [*m.n*]pyridinophanes (*m*, *n* = 2 or 3) showed sign inversions in their

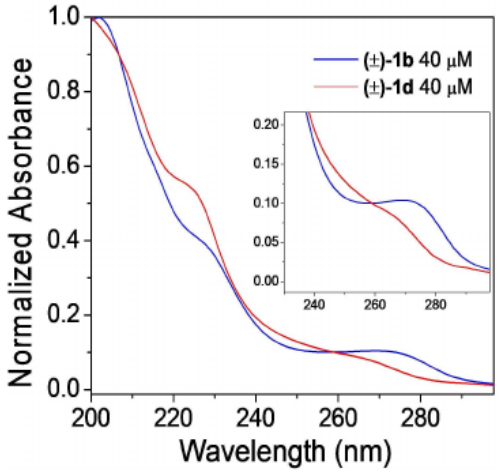

Figure 5. Normalized UV/Vis spectroscopy of (±)-**1b** and (±)-**1d** (40 μM) in MCH at 298 K and a magnification of the cyclophane band (inset).

CD spectra attributed to a change in the direction of the electronic transition dipole moment.[68][69] The major application of CD for supramolecular polymers is to monitor the formation of helical aggregates in solution. In the case of **[2.2]pCpTA**, the monomer and aggregate chromophores are both expected to be in a chiral environment, so a detailed study of both forms will be needed to assign CD signatures of the assembly. In addition, *Mori* and coworkers recently attributed detailed *Cotton* effects for **[2.2]pCp**-bromides to the substitution pattern.[70] It is envisioned that different *Cotton* effects would be observed for the planar-chiral compounds (R_p)-**1b** and (R_p)-**3** resulting from their transannular H-bonding properties. Transannular H-bond capable ps-*o*-bisamide (R_p)-**1b** and monoamide (R_p)-**3** have similar *Cotton* effects in the higher energy region, with (R_p)-**3** exhibiting a more intense absorbance in the cyclophane region (250–285 nm) compared to (R_p)-**1b** (*Figure 6*). The corresponding absorbance peaks for both π–π^* bands (236 nm for (R_p)-**1b**, 232 nm for (R_p)-**3**) and cyclophane bands (277 nm for (R_p)-**1b**, 268 nm for (R_p)-**3**) are bathochromically shifted for (R_p)-**3** compared to those in (R_p)-**1b**. The enantiomers ((S_p)-**1b** and (R_p)-**3**) give the expected mirror-image spectra (*Figure 6*). The CD spectra of amido-**[2.2]pCps** feature more peaks and fine-structure compared to the UV/Vis absorbance spectra and could be more sensitive to changes in aggregation. Both amido-**[2.2]pCps** studied are incapable of forming aggregates at these concentrations, but their chromophores are in a chiral environment in the monomeric state. Comparison to helical assemblies of **[2.2]pCpTA** will provide more information about intermonomer chromophore interactions.

Conclusions

In this work, **[2.2]pCp**-bisamide regioisomers were synthesized and their transannular and intermolecular hydrogen bonding properties characterized by IR, UV/Vis and NMR spectroscopy. The X-ray structure of (±)-**1a** maintains a transannular H-bond in the solid state, although unlike **[2.2]pCpTA**, no homochiral self-recognition is observed. In nonpolar solvents such as methylcyclohexane and (D_{12})cyclohexane, disordered aggregates of (±)-**1b** are formed. Importantly,

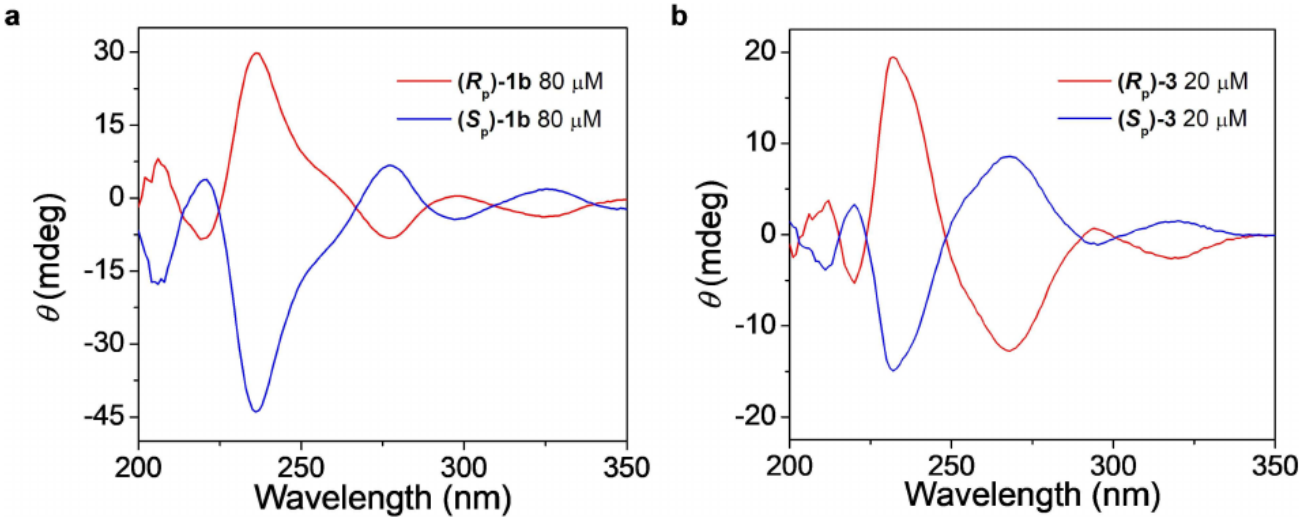

Figure 6. a) Circular dichroism spectra of (R_p)-**1b** (red) and (S_p)-**1b** (blue) (80 μM), and b) (R_p)-**1b** (red) and (S_p)-**1b** (blue) (20 μM), in MCH.

C_5–C_4–C_{17}–O_1 bond rotation is fast on the NMR timescale in solutions of both $CDCl_3$ and (D_{12})-cyclohexane. Studies of **[2.2]pCp**-bisamides have given evidence for possible pathway selection among self-assembling **[2.2]pCpTA**, as interconversion between *syn*- and *anti*-conformers is faster than the assembly timescale. Therefore, the assembly of **[2.2]-pCpTA** under thermodynamic control is likely comprised of the *anti*- conformer, and this hypothesis is consistent with recent computational investigations.[55]

The characterization of (±)-**1b** and alkylated comparator (±)-**1c** allowed the assignment of both intermolecular and transannularly H-bonded N–H stretches by IR. Comparison between H-bond capable (±)-**1b** and alkylated, H-bond incapable (±)-**1d** show the effects of transannular hydrogen bonding on the optical properties of **[2.2]pCp**-bisamides. Finally, optical resolution of **1b** and **3** was achieved for circular-dichroism studies in which both amido-**[2.2]pCps** showed similarly structured, well-defined *Cotton* effects through the UV and visible region. Extension of this analysis, including the chiral resolution protocol, to **[2.2]pCpTA** is underway.

Experimental Section

General

Characterization, instrumentation, methods, and materials are described in detail in the *Supporting Information*.

Previously Reported Compounds

(±)-4-(hexyl)amide[2.2]paracyclophane ((±)-**3**),[37] (±)-4,12-dicarboxy[2.2]paracyclophane ((±)-**4**),[71] 4,16-dicarboxy[2.2]paracyclophane (**5**),[72] (±)-4,12-dibromo-[2.2]paracyclophane ((±)-**6**),[16] and sulfinyl diastereoisomers (R_p,*S*)-**7** and (S_p,*S*)-**7**,[57] were prepared with slight modification to reported procedures as described in detail in the *Supporting Information*.

(±)-4,12-Di(propyl)amide[2.2]paracyclophane (=*N*^{5},*N*^{11}-dipropyltricyclo[8.2.2.2^{4,7}]hexadeca-1(12),4,6,10,13,15-hexaene-5,11-dicarboxamide; (±)-**1a**). Oxalyl chloride (0.10 mL, 1.2 mmol), was added to a suspension of (±)-**4** (43 mg, 0.15 mmol) in CH_2Cl_2 (15 mL). A catalytic amount of DMF (one drop) was added, and the solution was stirred at room temperature for 2 h. Solvent and excess reagent were removed by distillation, and the mixture was re-dissolved in CH_2Cl_2 (15 mL) and cooled to 0 °C with an ice water bath. *N*-Propylamine (0.13 mL, 1.0 mmol) and DIPEA (0.13 mL, 1.0 mmol) were added in one portion by syringe, and the mixture was warmed to room temperature over the course of 2 h. The mixture was diluted with CH_2Cl_2 and washed with 2 N HCl. The organic layer was dried with $MgSO_4$, filtered, and the solvent was removed *in vacuo*. The product was purified by silica gel chromatography (70% ethyl acetate in hexanes) to yield a sticky, colorless solid (21 mg, 39% yield). Crystallization by slow evaporation from MeOH yielded colorless plates suitable for single crystal X-ray diffraction. ^{1}H-NMR (500 MHz, $CDCl_3$): 7.35 (*t*, *J* = 6.2, 2 H); 6.86 (*s*, 2 H); 6.66–6.54 (*m*, 4 H); 3.80–3.66 (*m*, 2 H); 3.45 (*td*, *J* = 7.4, 5.8, 4 H); 3.19–3.05 (*m*, 2 H); 2.95–2.75 (*m*, 4 H); 1.73 (*m*, *J* = 7.3, 4 H); 1.05 (*t*, *J* = 7.4, 6 H). ^{13}C-NMR (126 MHz, $CDCl_3$): 169.52; 139.78; 137.77; 137.02; 135.75; 134.12; 129.71; 41.67; 34.58; 34.45; 22.79; 11.59. HR-ESI-MS: 379.2388 ($C_{24}H_{31}N_2O_2^+$, [*M* + H]$^+$; calc. 379.2380).

(±)-4,12-Di(hexyl)amide[2.2]paracyclophane (=*N*^{5},*N*^{11}-dihexyltricyclo[8.2.2.2^{4,7}]hexadeca-1(12),4,6,10,13,15-hexaene-5,11-dicarboxamide; (±)-**1b**). This compound was synthesized following the same method as (±)-**1a** using oxalyl chloride (0.10 mL, 1.2 mmol), (±)-**4** (72 mg, 0.24 mmol), hexylamine (0.13 mL, 1.0 mmol), and DIPEA (0.13 mL, 1.0 mmol) in CH_2Cl_2 (12 mL). The product was further purified by silica gel chromatography (40% ethyl acetate in hexanes) to yield a sticky, colorless solid (49 mg, 44% yield). ^{1}H-NMR (500 MHz, $CDCl_3$): 7.35 (*t*, *J* = 5.8, 2 H); 6.85 (*s*, 2 H); 6.60 (*q*, *J* = 6.8, 4 H); 3.77–3.66 (*m*, 2 H); 3.50–3.42 (*m*, 4 H); 3.18–3.07 (*m*, 2 H); 2.93–2.76 (*m*, 4 H); 1.74–1.64 (*m*, 4 H); 1.51–1.29 (*m*, 12 H); 0.95–0.86 (*m*, 6 H). ^{13}C-NMR (126 MHz, $CDCl_3$): 169.46; 139.77; 137.75; 137.06; 135.74; 134.09; 129.72; 39.94; 34.58; 34.45; 31.49; 29.45; 26.78; 22.56; 13.97. HR-ESI-MS: 463.3308 ($C_{30}H_{43}N_2O_2^+$, [*M* + H]$^+$; calc. 463.3319).

(±)-4-*N*-(Hexyl),*N*′-methyl-amide,12-(hexyl)amide-[2.2]paracyclophane (=*N*^{5},*N*^{11}-dihexyl-*N*^{5}-methyltricyclo[8.2.2.2^{4,7}]hexadeca-1(12),4,6,10,13,15-hexaene-5,11-dicarboxamide; (±)-**1c**). Compound (±)-**1b** (23 mg, 0.05 mmol) was stirred in anhydrous DMF (6 mL) with NaH 60% dispersion in mineral oil (3 mg, 0.8 mmol) for 1 h. MeI (50 μL, 0.75 mmol) was added and stirred for 15 min. The reaction was quenched with H_2O and extracted into ethyl acetate. The solution was dried with Na_2SO_4, and the solvent was removed *in vacuo*. The product was purified by silica gel chromatography (30–40% ethyl acetate in hexanes) to yield a colorless solid (18 mg, 78% yield). ^{1}H-NMR (500 MHz, $CDCl_3$): 9.10–8.91 (*m*, 1 H); 7.02 (*dd*, *J* = 14.8, 1.8, 1 H); 6.71–6.48 (*m*, 5 H);

4.04–3.94 (*m*, 1 H); 3.53 (*m*, 1 H); 3.44–3.33 (*m*, 1 H); 3.18–2.74 (*m*, 8 H); 2.69 (*s*, 1 H); 1.78–1.62 (*m*, 3 H); 1.53–1.17 (*m*, 11 H); 1.16–1.04 (*m*, 1 H); 1.03–0.78 (*m*, 6 H); 0.75 (*t*, *J*=7.3, 1 H). ^{13}C-NMR (126 MHz, $CDCl_3$): 172.34; 171.79; 169.06; 169.02; 141.17; 141.02; 139.85; 139.81; 138.86; 138.78; 138.12; 138.02; 136.47; 136.26; 135.57; 135.49; 134.90; 134.80; 134.57; 134.54; 133.89; 133.81; 133.64; 133.18; 129.96; 129.90; 128.61; 128.41; 50.49; 47.64; 40.04; 39.99; 36.39; 34.68; 34.62; 34.52; 34.43; 33.69; 33.63; 32.80; 31.88; 31.86; 31.78; 31.18; 29.85; 29.69; 29.65; 27.79; 27.21; 27.19; 27.11; 26.86; 25.96; 22.85; 22.84; 22.80; 22.48; 14.26; 14.20; 13.97. HR-ESI-MS: 477.3470 ($C_{31}H_{45}N_2O_2^+$, $[M+H]^+$; calc. 477.3456).

(±)-4,12-*N*,*N*′-Bis(dimethyl)amide[2.2]paracyclophane (=***N*^5^,*N*^5^,*N*^11^,*N*^11^-tetramethyltricyclo[8.2.2.2^4,7^]hexadeca-1(12),4,6,10,13,15-hexaene-5,11-dicarboxamide**; (±)-**1d**). This compound was synthesized following the same method as (±)-**1b** using oxalyl chloride (0.1 mL, 1.3 mmol), (±)-**4** (37 mg, 0.13 mmol), dimethylamine (40% aq.) heated and bubbled in using a cannula, and DIPEA (0.13 mL, 1.0 mmol) in CH_2Cl_2 (12 mL). The product was purified by silica gel chromatography (100% ethyl acetate) to yield a white powder (22 mg, 49% yield). ^{1}H-NMR (500 MHz, $CDCl_3$): 7.01 (*t*, *J*=1.6, 2 H); 6.64–6.50 (*m*, 4 H); 3.30–3.13 (*m*, 6 H); 3.02 (*s*, 10 H); 2.80 (*m*, 2 H); 2.56 (*s*, 6 H). ^{13}C-NMR (126 MHz, $CDCl_3$): 171.13; 139.82; 138.09; 134.17; 134.06; 131.59; 130.26; 38.65; 34.81; 34.19. HR-ESI-MS: 351.2056 ($C_{22}H_{27}N_2O_2^+$, $[M+H]^+$; calc. 351.2067).

4,16-Di(hexyl)amide[2.2]paracyclophane (=***N*^5^,*N*^11^-dihexyltricyclo[8.2.2.2^4,7^]hexadeca-1(12),4,6,10,13,15-hexaene-5,11-dicarboxamide**; **2**). This compound was synthesized following the same method as (±)-**1b** using oxalyl chloride (0.03 mL, .31 mmol), **5** (21 mg, 0.08 mmol), hexylamine (0.13 mL, 1.0 mmol), and DIPEA (0.13 mL, 1.0 mmol) in CH_2Cl_2 (12 mL). The product was purified by silica gel chromatography (40% ethyl acetate in hexanes) to yield a colorless, crystalline solid (16 mg, 44% yield). ^{1}H-NMR (500 MHz, $CDCl_3$): 6.93 (*d*, *J*=7.9, 2 H); 6.67 (*s*, 2 H); 6.41 (*d*, *J*=7.8, 2 H); 5.58–5.40 (*m*, 2 H); 3.62 (*t*, *J*=2.0, 2 H); 3.50–3.23 (*m*, 6 H); 2.95 (*m*, 4 H); 1.59 (*dd*, *J*=14.0, 6.7, 6 H); 1.33 (*dd*, *J*=7.3, 3.9, 14 H); 0.94–0.85 (*m*, 6 H). ^{13}C-NMR (126 MHz, $CDCl_3$): 169.70; 140.49; 138.54; 135.34; 135.32; 134.06; 131.29; 39.99; 35.09; 33.92; 31.64; 29.87; 26.86; 22.74; 14.17. HR-ESI-MS: 463.3341 ($C_{30}H_{43}N_2O_2^+$, $[M+H]^+$; calc. 463.3319).

Supplementary Material

CCDC-1895863 contains the supplementary crystallographic data for this work. These data can be obtained free of charge from *The Cambridge Crystallographic Data Centre via* www.ccdc.cam.ac.uk/data_request/cif.

Acknowledgements

Acknowledgement is made to the Donors of the *American Chemical Society Petroleum Research Fund* for support of this research (PRF #56665-ND4). Additional support for *J. G.* is acknowledged from the *National Science Foundation REU* program (CHE-1156907). *K. A. A.* wishes to acknowledge the *National Science Foundation* and the University of Florida for funding of the purchase of the X-ray equipment.

Author Contribution Statement

W. R. H., D. E. F. and *J. G.* performed the synthesis and characterization of all materials. *K. A. A.* performed X-ray crystallographic analysis. *W. R. H.* and *D. E. F.* performed NMR and IR experiments and analysis. *W. R. H.* did the remainder of experiments. *R. K. C.* designed experiments and supervised. *W. R. H., D. E. F.,* and *R. K. C.* wrote the manuscript.

References

[1] Z. Hassan, E. Spuling, D. M. Knoll, J. Lahann, S. Bräse, 'Planar chiral [2.2]paracyclophanes: from synthetic curiosity to applications in asymmetric synthesis and materials', *Chem. Soc. Rev.* **2018**, *47*, 6947–6963.

[2] H. Hopf, '[2.2]Paracyclophanes in Polymer Chemistry and Materials Science', *Angew. Chem. Int. Ed.* **2008**, *47*, 9808–9812.

[3] R. Gleiter, H. Hopf, 'Modern Cyclophane Chemistry', Wiley-VCH, Weinheim, 2004.

[4] D. J. Cram, J. M. Cram, 'Cyclophane Chemistry: Bent and Battered Benzene Rings', *Acc. Chem. Res.* **1971**, *4*, 204–213.

[5] M. Gon, Y. Morisaki, Y. Chujo, 'Optically active cyclic compounds based on planar chiral [2.2]paracyclophane: extension of the conjugated systems and chiroptical properties', *J. Mater. Chem. C* **2015**, *3*, 521–529.

[6] M. Gon, R. Sawada, Y. Morisaki, Y. Chujo, 'Enhancement and Controlling the Signal of Circularly Polarized Luminescence Based on a Planar Chiral Tetrasubstituted [2.2] Paracyclophane Framework in Aggregation System', *Macromolecules* **2017**, *50*, 1790–1802.

[7] E. Benedetti, M.-L. Delcourt, B. Gatin-Fraudet, S. Turcaud, L. Micouin, 'Synthesis and photophysical studies of through-

space conjugated [2.2]paracyclophane-based naphthalene fluorophores', *RSC Adv.* **2017**, *7*, 50472–50476.
[8] Y. Sasai, H. Tsuchida, T. Kakuta, T. Ogoshi, Y. Morisaki, 'Synthesis of optically active π-stacked compounds based on planar chiral tetrasubstituted [2.2]paracyclophane', *Mater. Chem. Front.* **2018**, *2*, 791–795.
[9] W. J. Oldham Jr., Y.-J. Miao, R. Lachicotte, G. C. Bazan, 'Stilbenoid Dimers: Effect of Conjugation Length and Relative Chromophore Orientation', *J. Am. Chem. Soc.* **1998**, *120*, 419–420.
[10] G. P. Bartholomew, I. Ledoux, S. Mukamel, G. C. Bazan, J. Zyss, 'Three-Dimensional Nonlinear Optical Chromophores Based on Through-Space Delocalization', *J. Am. Chem. Soc.* **2002**, *124*, 13480–13485.
[11] J. W. Hong, B. S. Gaylord, G. C. Bazan, 'Water-Soluble Oligomer Dimers Based on Paracyclophane: A New Optical Platform for Fluorescent Sensor Applications', *J. Am. Chem. Soc.* **2002**, *124*, 11868–11869.
[12] A. Ruseckas, E. B. Namdas, J. Y. Lee, S. Mukamel, S. Wang, G. C. Bazan, V. Sundström, 'Conformations and Photophysics of a Stilbene Dimer', *J. Phys. Chem. A* **2003**, *107*, 8029–8034.
[13] J. W. Hong, H. Y. Woo, B. Liu, G. C. Bazan, 'Solvatochromism of Distyrylbenzene Pairs Bound Together by [2.2]Paracyclophane: Evidence for a Polarizable "Through-Space" Delocalized State', *J. Am. Chem. Soc.* **2005**, *127*, 7435–7443.
[14] H. Y. Woo, J. W. Hong, B. Liu, A. Mikhailovsky, D. Korystov, G. C. Bazan, 'Water-Soluble [2.2]Paracyclophane Chromophores with Large Two-Photon Action Cross Sections', *J. Am. Chem. Soc.* **2005**, *127*, 820–821.
[15] A. M. Moran, J. B. Maddox, J. W. Hong, J. Kim, R. A. Nome, G. C. Bazan, S. Mukamel, N. F. Scherer, 'Optical coherence and theoretical study of the excitation dynamics of a highly symmetric cyclophane-linked oligophenylenevinylene dimer', *J. Chem. Phys.* **2006**, *124*, 194904.
[16] H. J. Reich, D. J. Cram, 'Macro Rings. XXXVII. Multiple Electrophilic Substitution Reactions of [2.2]Paracyclophanes and Interconversions of Polysubstituted Derivatives', *J. Am. Chem. Soc.* **1969**, *91*, 3527–3533.
[17] H. J. Reich, D. J. Cram, 'Macro Rings. XXXVI. Ring Expansion, Racemization, and Isomer Interconversions in the [2.2]Paracyclophane System through a Diradical Intermediate', *J. Am. Chem. Soc.* **1969**, *91*, 3517–3526.
[18] S. Kotha, M. E. Shirbhate, G. T. Waghule, 'Selected synthetic strategies to cyclophanes', *Beilstein J. Org. Chem.* **2015**, *11*, 1274–1331.
[19] A. A. Aly, A. B. Brown, 'Asymmetric and fused heterocycles based on [2.2]paracyclophane', *Tetrahedron* **2009**, *65*, 8055–8089.
[20] D. K. Whelligan, C. Bolm, 'Synthesis of Pseudo-*geminal*-, Pseudo-*ortho*-, and *ortho*-Phosphinyl-oxazolinyl-[2.2]paracyclophanes for Use as Ligands in Asymmetric Catalysis', *J. Org. Chem.* **2006**, *71*, 4609–4618.
[21] P. J. Pye, K. Rossen, R. A. Reamer, N. N. Tsou, R. P. Volante, P. J. Reider, 'New Planar Chiral Bisphosphine Ligand for Asymmetric Catalysis: Highly Enantioselective Hydrogenations under Mild Conditions', *J. Am. Chem. Soc.* **1997**, *119*, 6207–6208.
[22] M. Kreis, C. J. Friedmann, S. Bräse, 'Diastereoselective Hartwig–Buchwald Reaction of Chiral Amines with *rac*-[2.2]Paracyclophane Derivatives', *Chem. Eur. J.* **2005**, *11*, 7387–7394.
[23] Y. Morisaki, N. Wada, M. Arita, Y. Chujo, 'Synthesis of through-space conjugated polymers containing the pseudo-*ortho*-linked [2.2]paracyclophane moiety', *Polym. Bull.* **2009**, *62*, 305–314.
[24] Y. Morisaki, Y. Chujo, 'Through-Space Conjugated Polymers', in 'Conjugated Polymer Synthesis: Methods and Reactions', Ed. Y. Chujo,Wiley-VCH, Weinheim, 2010, pp. 133–163.
[25] Y. Morisaki, R. Hifumi, L. Lin, K. Inoshita, Y. Chujo, 'Through-space conjugated polymers consisting of planar chiral pseudo-*ortho*-linked [2.2]paracyclophane', *Polym. Chem.* **2012**, *3*, 2727–2730.
[26] M. Wielopolski, A. Molina-Ontoria, C. Schubert, J. T. Margraf, E. Krokos, J. Kirschner, A. Gouloumis, T. Clark, D. M. Guldi, N. Martín, 'Blending Through-Space and Through-Bond π–π-Coupling in [2,2′]-Paracyclophane-oligophenylenevinylene Molecular Wires', *J. Am. Chem. Soc.* **2013**, *135*, 10372–10381.
[27] Y. Morisaki, K. Inoshita, Y. Chujo, 'Planar-Chiral Through-Space Conjugated Oligomers: Synthesis and Characterization of Chiroptical Properties', *Chem. Eur. J.* **2014**, *20*, 8386–8390.
[28] Y. J. Chang, M. Watanabe, P.-T. Chou, T. J. Chow, '[2.2]Paracyclophane as a bridging unit in the design of organic dyes for sensitized solar cells', *Chem. Commun.* **2012**, *48*, 726–728.
[29] Y. Morisaki, Y. Chujo, 'Through-Space Conjugated Polymers Based on Cyclophanes', *Angew. Chem. Int. Ed.* **2006**, *45*, 6430–6437.
[30] F. Diederich, D. R. Carcanague, 'A Spacious Cyclophane Host for Inclusion Complexation of Steroids and [m.n]Paracyclophanes', *Angew. Chem. Int. Ed.* **1990**, *29*, 769–771.
[31] S. Anderson, U. Neidlein, V. Gramlich, F. Diederich, 'A New Family of Chiral Binaphthyl-Derived Cyclophane Receptors: Complexation of Pyranosides', *Angew. Chem. Int. Ed.* **1995**, *34*, 1596–1600.
[32] S. B. Ferguson, E. M. Sanford, E. M. Seward, F. Diederich, 'Cyclophane Arene Inclusion Complexation in Protic Solvents: Solvent Effects versus Electron Donor–Acceptor Interactions', *J. Am. Chem. Soc.* **1991**, *113*, 5410–5419.
[33] F. Diederich, 'Complexation of Neutral Molecules by Cyclophane Hosts', *Angew. Chem. Int. Ed.* **1988**, *27*, 362–386.
[34] H. Hopf, S. V. Narayanan, P. G. Jones, 'The preparation of new functionalized [2.2]paracyclophane derivatives with *N*-containing functional groups', *Beilstein J. Org. Chem.* **2015**, *11*, 437–445.
[35] J. F. Schneider, R. Fröhlich, J. Paradies, '[2.2]Paracyclophane-Derived Planar-Chiral Hydrogen-Bond Receptors', *Isr. J. Chem.* **2012**, *52*, 76–91.
[36] E. Elacqua, T. Friščić, L. R. MacGillivray, '[2.2]Paracyclophane as a Target of the Organic Solid State: Emergent Properties via Supramolecular Construction', *Isr. J. Chem.* **2012**, *52*, 53–59.
[37] D. E. Fagnani, M. J. Meese Jr., K. A. Abboud, R. K. Castellano, 'Homochiral [2.2]Paracyclophane Self-Assembly Promoted by Transannular Hydrogen Bonding', *Angew. Chem. Int. Ed.* **2016**, *55*, 10726–10731.

[38] M. L. Bushey, T.-Q. Nguyen, W. Zhang, D. Horoszewski, C. Nuckolls, 'Using Hydrogen Bonds to Direct the Assembly of Crowded Aromatics', *Angew. Chem. Int. Ed.* **2004**, *43*, 5446–5453.
[39] R. K. Castellano, 'Special Issue: Intramolecular Hydrogen Bonding', *Molecules* **2014**, *19*, 15783–15785.
[40] G. P. Dado, S. H. Gellman, 'Intramolecular Hydrogen Bonding in Derivatives of β-Alanine and γ-Amino Butyric Acid; Model Studies for the Folding of Unnatural Polypeptide Backbones', *J. Am. Chem. Soc.* **1994**, *116*, 1054–1062.
[41] D.-W. Zhang, X. Zhao, J.-L. Hou, Z.-T. Li, 'Aromatic Amide Foldamers: Structures, Properties, and Functions', *Chem. Rev.* **2012**, *112*, 5271–5316.
[42] C. Bilton, F. H. Allen, G. P. Shields, J. A. Howard, 'Intramolecular hydrogen bonds: common motifs, probabilities of formation and implications for supramolecular organization', *Acta Crystallogr. B* **2000**, *56*, 849–856.
[43] Y. Liu, J. Shen, C. Sun, C. Ren, H. Zeng, 'Intramolecularly Hydrogen-Bonded Aromatic Pentamers as Modularly Tunable Macrocyclic Receptors for Selective Recognition of Metal Ions', *J. Am. Chem. Soc.* **2015**, *137*, 12055–12063.
[44] F. H. Beijer, R. P. Sijbesma, H. Kooijman, A. L. Spek, E. W. Meijer, 'Strong Dimerization of Ureidopyrimidones via Quadruple Hydrogen Bonding', *J. Am. Chem. Soc.* **1998**, *120*, 6761–6769.
[45] X. Zhao, Z.-T. Li, 'Hydrogen bonded aryl amide and hydrazide oligomers: a new generation of preorganized soft frameworks', *Chem. Commun.* **2010**, *46*, 1601–1616.
[46] J. Alvarez, M. Gómez-Kaifer, 'Importance of intramolecular hydrogen bonding for preorganization and binding of molecular guests by water-soluble calix[6]arene hosts', *Chem. Commun.* **1998**, 1455–1456.
[47] T. Ogoshi, K. Kitajima, T. Aoki, T.-a. Yamagishi, Y. Nakamoto, 'Effect of an Intramolecular Hydrogen Bond Belt and Complexation with the Guest on the Rotation Behavior of Phenolic Units in Pillar[5]arenes', *J. Phys. Chem. Lett.* **2010**, *1*, 817–821.
[48] P. A. Gale, J. W. Steed, 'Supramolecular Chemistry: From Molecules to Nanomaterials', Vol. 8, Wiley Online Library, 2012.
[49] C. Beemelmanns, R. Husmann, D. K. Whelligan, S. Özçubukçu, C. Bolm, 'Planar-Chiral Bis-silanols and Diols as H-Bonding Asymmetric Organocatalysts', *Eur. J. Org. Chem.* **2012**, 3373–3376.
[50] S. Kitagaki, T. Ueda, C. Mukai, 'Planar chiral [2.2]paracyclophane-based bis(thiourea) catalyst: application to asymmetric Henry reaction', *Chem. Commun.* **2013**, *49*, 4030–4032.
[51] D. C. Braddock, I. D. MacGilp, B. G. Perry, 'Planar Chiral PHANOLs as Organocatalysts for the Diels-Alder Reaction via Double Hydrogen-Bonding to a Carbonyl Group', *Synlett* **2003**, 1121–1124.
[52] D. C. Braddock, I. D. MacGilp, B. G. Perry, 'Improved Synthesis of (±)-4,12-Dihydroxy[2.2]paracyclophane and Its Enantiomeric Resolution by Enzymatic Methods: Planar Chiral (*R*)-and (*S*)-Phanol', *J. Org. Chem.* **2002**, *67*, 8679–8681.
[53] C. Braun, S. Bräse, L. L. Schafer, 'Planar-Chiral [2.2]Paracyclophane-Based Amides as Proligands for Titanium- and Zirconium-Catalyzed Hydroamination', *Eur. J. Org. Chem.* **2017**, 1760–1764.
[54] A. Sorrenti, J. Leira-Iglesias, A. J. Markvoort, T. F. A. de Greef, T. M. Hermans, 'Non-equilibrium supramolecular polymerization', *Chem. Soc. Rev.* **2017**, *46*, 5476–5490.
[55] D. B. B. Korlepara, W. R. Henderson, R. K. Castellano, S. Balasubramanian, 'Differentiating the Mechanism of Self-Assembly in Supramolecular Polymers through Computation', *Chem. Commun.* **2019**, accepted manuscript, DOI: 10.1039/c9cc01058k.
[56] C. Kulkarni, S. Balasubramanian, S. J. George, 'What Molecular Features Govern the Mechanism of Supramolecular Polymerization?', *ChemPhysChem* **2013**, *14*, 661–673.
[57] Y. Morisaki, R. Hifumi, L. Lin, K. Inoshita, Y. Chujo, 'Practical Optical Resolution of Planar Chiral Pseudo-*ortho*-disubstituted [2.2]Paracyclophane', *Chem. Lett.* **2012**, *41*, 990–992.
[58] D. Y. Antonov, V. I. Rozenberg, T. I. Danilova, Z. A. Starikova, H. Hopf, 'Iminophenol Ligands Derived from Chiral Regioisomeric Hydroxy[2.2]paracyclophane-carbaldehydes: the Influence of the Substitution Pattern on Asymmetric Induction', *Eur. J. Org. Chem.* **2008**, 1038–1048.
[59] I. Dix, L. Bondarenko, P. G. Jones, L. Ernst, K. Ibrom, J. Grunenberg, R. Boese, H. Hopf, 'Preparation, Structural Properties and Thermal Isomerization of Hex-3-ene-1,5-diyne Bridged [2.2]Paracyclophanes', *Chem. Eur. J.* **2014**, *20*, 16360–16376.
[60] V. A. Davankov, 'The nature of chiral recognition: Is it a three-point interaction?', *Chirality* **1997**, *9*, 99–102.
[61] S. E. Walden, D. T. Glatzhofer, 'Distinctive Normal Harmonic Vibrations of [2.2]Paracyclophane', *J. Phys. Chem. A* **1997**, *101*, 8233–8241.
[62] K. Sako, T. Hasegawa, H. Onda, M. Shiotsuka, M. Watanabe, T. Shinmyozu, S. Tojo, M. Fujitsuka, T. Majima, Y. Hirao, T. Kubo, T. Iwanaga, S. Toyota, H. Takemura, 'Donor–Donor′–Acceptor Triads Based on [3.3]Paracyclophane with a 1,4-Dithiafulvene Donor and a Cyanomethylene Acceptor: Synthesis, Structure, and Electrochemical and Photophysical Properties', *Chem. Eur. J.* **2018**, *24*, 11407–11416.
[63] T. Miyazaki, M. Shibahara, J. Fujishige, M. Watanabe, K. Goto, T. Shinmyozu, 'Synthesis and Electronic and Photophysical Properties of [2.2]- and [3.3]Paracyclophane-Based Donor–Donor′–Acceptor Triads', *J. Org. Chem.* **2014**, *79*, 11440–11453.
[64] G. P. Bartholomew, G. C. Bazan, 'Bichromophoric Paracyclophanes: Models for Interchromophore Delocalization', *Acc. Chem. Res.* **2001**, *34*, 30–39.
[65] G. C. Bazan, W. J. Oldham Jr., R. J. Lachicotte, S. Tretiak, V. Chernyak, S. Mukamel, 'Stilbenoid Dimers: Dissection of a Paracyclophane Chromophore', *J. Am. Chem. Soc.* **1998**, *120*, 9188–9204.
[66] T. Mori, Y. Inoue, S. Grimme, 'Quantum Chemical Study on the Circular Dichroism Spectra and Specific Rotation of Donor- Acceptor Cyclophanes', *J. Phys. Chem. A* **2007**, *111*, 7995–8006.
[67] T. Furo, T. Mori, T. Wada, Y. Inoue, 'Absolute Configuration of Chiral [2.2]Paracyclophanes with Intramolecular Charge-Transfer Interaction. Failure of the Exciton Chirality Method and Use of the Sector Rule Applied to the Cotton Effect of the CT Transition', *J. Am. Chem. Soc.* **2005**, *127*, 8242–8243.
[68] A. Shimizu, Y. Inoue, T. Mori, 'Protonation-Induced Sign Inversion of the Cotton Effects of Pyridinophanes. A Combined Experimental and Theoretical Study', *J. Phys. Chem. A* **2017**, *121*, 977–985.

[69] A. Shimizu, Y. Inoue, T. Mori, 'A Combined Experimental and Theoretical Study on the Circular Dichroism of Staggered and Eclipsed Forms of Dimethoxy[2.2]-, [3.2]-, and [3.3]Pyridinophanes and Their Protonated Forms', *J. Phys. Chem. A* **2017**, *121*, 8389–8398.
[70] M. Toda, Y. Inoue, T. Mori, 'Circular Dichroisms of Mono- and Dibromo[2.2]paracyclophanes: A Combined Experimental and Theoretical Study', *ACS Omega* **2018**, *3*, 22–29.
[71] D. Y. Antonov, E. V. Sergeeva, E. V. Vorontsov, V. I. Rozenberg, 'Synthesis of [2.2]paracyclophane-*pseudo*-*ortho*-dicarboxylic acid', *Russ. Chem. Bull.* **1997**, *46*, 1897–1900.
[72] V. Kumar, S. Chatterjee, P. Sharma, S. Chakrabarty, C. V. Avadhani, S. Sivaram, 'Soluble polybenzimidazoles with intrinsic porosity: Synthesis, structure, properties and processability', *J. Polym. Sci. Part A* **2018**, *56*, 1046–1057.

Received February 7, 2019
Accepted March 7, 2019

